A Large Along-Track Baseline Approach for Ground Moving Target Indication Using TanDEM-X

Stefan V. Baumgartner, Gerhard Krieger, Karl-Heinz Bethke
Microwaves and Radar Institute, German Aerospace Center (DLR)
Muenchner Straße 20, 82234 Weßling, GERMANY
Email: stefan.baumgartner@dlr.de

***Abstract*— In the paper a new method for ground moving target indication using two satellites (i.e. the TerraSAR-X and the TanDEM-X satellite) is presented. For this special method the along-track baseline between the satellites is chosen to be in the order of several kilometres, so that each satellite observes the same moving target at different times. The proposed method allows the estimation of the true broadside position of the moving target with high accuracy as well as the estimation of the ground velocity and acceleration vector without the need of complex bistatic processing techniques.**

Keywords – Ground moving target indication (GMTI), along-track interferometry (ATI), TerraSAR-X, TanDEM-X

I. INTRODUCTION

The German TanDEM-X [1] mission concept is based on an extension of the TerraSAR-X mission by a second TerraSAR-X like satellite with the main goal of generating a world-wide high-precision digital elevation model (DEM). Both satellites will fly in close formation and will be operated as a flexible single-pass SAR interferometer where the baseline can be selected nearly arbitrarily. The first satellite, TerraSAR-X, was already launched in June 2007 and the second one, TanDEM-X, will be launched in 2009.

In the paper a method for ground moving target indication (GMTI) using both satellites together is presented. For this special method, the along-track baseline between the satellites is chosen to be in the order of several kilometres, corresponding to a time lag of a few seconds. Hence, the moving vehicles on ground are observed from both satellites at different times. For that reason, the displacements of the moving vehicles in both commonly processed SAR images will be different due to the time lag and the vehicle motion.

Each of the satellites will be operated in the so called dual receive antenna (DRA) mode, where the receiving antenna is divided in the along-track direction into two independent parts for data acquisition, thus enabling the application of the displaced phase center antenna (DPCA) technique for clutter suppression [2]. Instead of using the DRA mode for generating two independent receiving channels on each satellite, also aperture switching techniques can be used for the same purpose [3].

By applying common two-dimensional correlation or tracking methods the relative target displacements between both clutter suppressed DPCA images can be estimated. In the manuscript the mathematical relationships between these relative displacements and the moving targets motion parameters are derived and verified using a SAR GMTI simulator.

II. MATHEMATICAL RELATIONSHIP OF RELATIVE TARGET DISPLACEMENTS

For the following investigations the Cartesian radar geometry shown in Fig. 1 is considered. The SAR platform moves with constant velocity v_p in along-track direction. The instantaneous motion parameters of the moving target at broadside time $t = 0$, where the target is located at $x = x_1 = 0$, $y = y_1$ and $z = 0$ are: along-track velocity v_{x1}, across-track velocity v_{y1}, along-track acceleration a_x and across-track acceleration a_y. The target doesn't move in z-direction and it is assumed that the acceleration components remain constant during the whole observation interval.

The along-track displacement Δx_1 of the moving target image after common SAR processing for the non-squinted and Nyquist sampled case is given as [4]:

$$\Delta x_1 \cong -v_p \frac{f_{DC,1}}{k_{a,1}}, \tag{1}$$

where $f_{DC,1}$ is the Doppler shift and $k_{a,1}$ is the Doppler slope of the received moving target signal. The Doppler shift and the Doppler slope in the spaceborne case ($v_p >> v_{x1}$, v_{y1}, short observation time in the order of one second) can be approximated as :

$$f_{DC,1} \cong -\frac{2}{\lambda}\frac{y_1}{r_1}v_{y1} = -\frac{2}{\lambda}v_{y1}\sin\theta_{i,1}\ , \tag{2}$$

$$k_{a,1} \cong -\frac{2}{\lambda r_1}\left[\left(v_p - v_{x1}\right)^2 + y_1 a_y\right], \qquad (3)$$

where r_1 is the slant range distance at $t = 0$, y_1 the across-track distance at $t = 0$, $\theta_{i,1}$ the incidence angle and λ the radar wavelength. Due to common chirp scaling processing for the stationary case, the image of the moving target is also shifted in across-track direction by

$$\Delta y_1 \cong \frac{\Delta x_1}{2v_p} v_{y1} = \frac{1}{\lambda k_{a,1}} \frac{y_1}{r_1} v_{y1}^{\,2} = \frac{\sin\theta_{i,1}}{\lambda k_{a,1}} v_{y1}^{\,2} \,. \qquad (4)$$

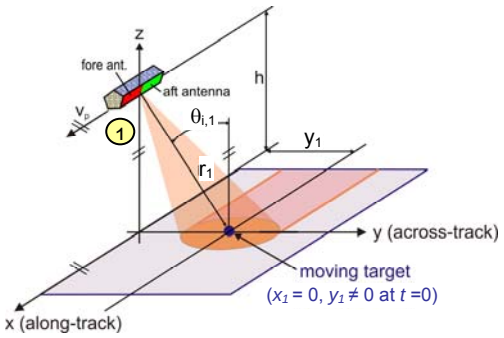

Figure 1. Two-channel side-looking radar geometry.

Considering now a second radar platform, displaced only in along-track direction about d_a from the first one as shown in Fig. 2.

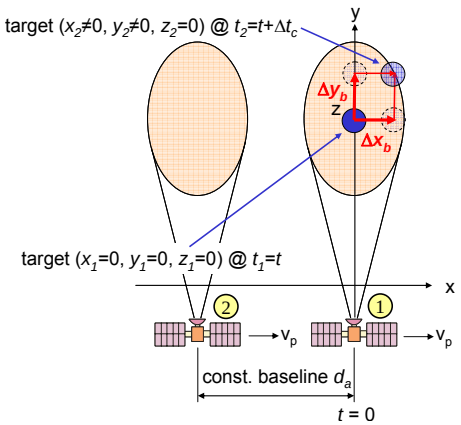

Figure 2. Satellite along-track configuration.

For co-registering (with respect to stationary targets) the data acquired from platform 2 with the data from platform 1, a time shift of $\Delta t_c = -d_a/v_p$ is necessary. At $t = 0$ the moving target is at broadside of the first platform. The time difference Δt_b when the target is at broadside of the second platform is given as $\Delta t_b = d_a/\left(v_p - \bar{v}_x\right)$, where $\bar{v}_x$ is the average along-track velocity of the moving target during the time interval Δt_b. Since in the spaceborne case $v_p >> \bar{v}_x$, the times $|\Delta t_c|$ and $|\Delta t_b|$ differ only in a few milliseconds. During that short time difference the ground moving target in most practical cases will not travel through one full azimuth (along-track) resolution cell, so that the approximation $|\Delta t_b| \cong |\Delta t_c|$ can be used in all following equations.

During the time interval Δt_b the target travels on ground the following distances (cf. Fig. 2):

$$\Delta x_b = v_{x1}\Delta t_b + \frac{1}{2} a_x \Delta t_b^{\,2} = \bar{v}_x \Delta t_b \,, \qquad (5)$$

$$\Delta y_b = v_{y1}\Delta t_b + \frac{1}{2} a_y \Delta t_b^{\,2} = \bar{v}_y \Delta t_b \,. \qquad (6)$$

Note that the distances Δx_b and Δy_b in general are not the same as the relative target displacements Δx_{img} and Δy_{img} in the focused SAR images.

The relative along-track displacement of the moving target between both co-registered and focused SAR or DPCA images (cf. Fig. 3), respectively, can be expressed as (note that the parameters indexed with '2' correspond to the moving target signal received by the second SAR platform, i.e. that are the parameters of the target when it is at broadside of the second platform):

$$\Delta x_{img} = \Delta x_2 - \Delta x_1 = -v_p \frac{f_{DC,2}}{k_{a,2}} + \Delta x_b + v_p \frac{f_{DC,1}}{k_{a,1}} \,. \qquad (7)$$

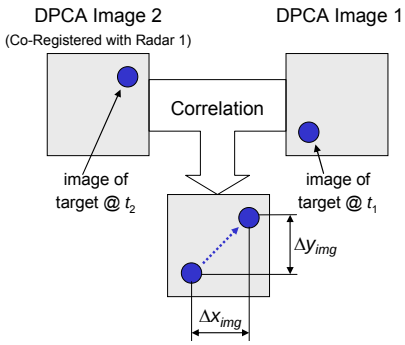

Figure 3. Relative target displacement in SAR or DPCA image domain, respectively.

If the along-track baseline between both satellites corresponds to a time lag of only a few seconds, the incidence angle and the Doppler slope of the moving target signal will not change significantly between both observations so that the following approximations are valid:

$$k_{a,1} \cong k_{a,2} = k_a \quad \text{and} \quad \theta_{i,1} \cong \theta_{i,2} \cong \theta_i \,. \qquad (8)$$

Using above approximations, equation (7) can be rewritten as:

$$\Delta x_{img} \cong v_p \frac{2\sin\theta_{i,1}}{\lambda k_{a,1}} a_y \Delta t_b + \Delta x_b = \Delta x_{img,ay} + \Delta x_b \,. \qquad (9)$$

Using the same approximations as before, the relative across-track displacement of the moving target images is then given by:

$$\Delta y_{img} = \Delta y_2 - \Delta y_1 \cong \frac{\sin\theta_{i,1}}{\lambda k_{a,1}} \Delta t_b \left(2 v_{y1} a_y + a_y^{\,2} \Delta t_b\right) + \Delta y_b \,. \qquad (10)$$

Since in most practical cases and real traffic scenarios [8] the first term of equation (10) is in the order or even smaller than one across-track resolution cell (at least for

TerraSAR-X and TanDEM-X geometries and stripmap system parameters), the across-track displacement can be approximated as:

$$\Delta y_{img} \cong \Delta y_b \tag{11}$$

All displacements expressed by previous equations are exemplary sketched in the time-frequency plane in Fig. 4 for visualization purposes and better appreciation. Note that the displacement $\Delta x_{img,ay}$ caused by the across-track acceleration a_y may be quite larger than the distance Δx_b traveled by the target during the interval Δt_b.

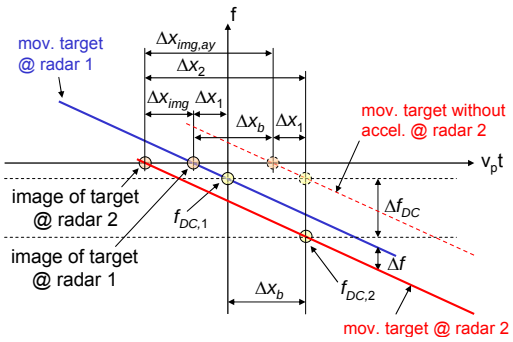

Figure 4. Displacements of co-registered signals in the time-frequency domain.

III. Parameter Estimation Procedure

Since both of the satellites, TerraSAR-X as well as TanDEM-X, have two receiving antennas, clutter suppression can be performed for each satellite independently using the DPCA technique. As result two independent DPCA images are obtained. Assuming that the moving target can be detected at least in one of the DPCA images (e.g. image 1 for the following investigations), the Doppler slope $k_{a,1}$ can be estimated for example by using a matched filter bank or the fractional Fourier transform [6]. Once the Doppler slope $k_{a,1}$ is known, each DPCA image can be refocused (cf. equation (8) $\rightarrow k_{a,1} \cong k_{a,2}$) to increase the SCNR.

The relative displacements Δx_{img} and Δy_{img} can be found e.g. by a two-dimensional correlation procedure (cf. Fig. 3). To increase computational speed, the searching area might be reduced by taking into account the along-track baseline d_a or the time Δt_c ($\cong \Delta t_b$), respectively and the maximum values of the expected target velocities and accelerations.

In equation (9) at the first term the Doppler slope $k_{a,1}$ is in the denominator and the value of this term is mainly determined by the product $a_y \Delta t_b$. A change of the Doppler slope of several Hz (i.e. due to the motion of the moving target) does not affect the whole term significantly so that as a good approximation the Doppler slope of a stationary target can be used instead of the motion dependent slope. Thus, (9) can be rewritten as (in the following all estimates are denoted with the "^" symbol):

$$\Delta\hat{x}_{img} \cong -\frac{r_1 \sin\theta_{i,1}}{v_p}\hat{a}_y \Delta t_b + \hat{\bar{v}}_x \Delta t_b \tag{12}$$

and the average along-track velocity can then be expressed by rewriting above equation:

$$\hat{\bar{v}}_x = \frac{\Delta\hat{x}_{img}}{\Delta t_b} + \frac{r_1 \sin\theta_{i,1}}{v_p}\hat{a}_y . \tag{13}$$

This average along-track velocity can be inserted in (3) instead of v_{x1}. Only a small mistake is made, since the effect caused by the small difference between $\bar{v}_x$ and v_{x1} is negligible compared to the product $y_1 a_y$. As result for the across-track acceleration a_y a quadratic equation is obtained:

$$\hat{a}_y^2 + \hat{a}_y p + q = 0 . \tag{14}$$

The parameters p and q are given as:

$$\begin{aligned} p &= \left(2AB - 2Bv_p + y_1\right)\frac{1}{B^2}, \\ q &= \left[\left(A - v_p\right)^2 + \frac{\lambda r_1 k_{a,1}}{2}\right]\frac{1}{B^2}, \end{aligned} \tag{15}$$

with

$$A = \frac{\Delta\hat{x}_{img}}{\Delta t_b}, \quad B = \frac{r_1 \sin\theta_{i,1}}{v_p}. \tag{16}$$

Due to physical reasons only the following solution of the quadratic equation (14) is of relevance:

$$\hat{a}_y = -\frac{p}{2} - \sqrt{\left(\frac{p}{2}\right)^2 - q} . \tag{17}$$

Using equation (6) with (11) the estimate of the across-track velocity is given as:

$$\hat{v}_{y1} = \frac{\Delta\hat{y}_{img}}{\Delta t_b} - \frac{1}{2}\hat{a}_y \Delta t_b . \tag{18}$$

With equation (1), (2) and (3) the value for repositioning the moving target in along-track direction in image 1 can be computed:

$$\Delta\hat{x}_{1,redisp} = -\Delta\hat{x}_1 \cong -\frac{2 v_p \sin\theta_{i,1}}{\lambda \hat{k}_{a,1}}\hat{v}_{y1} . \tag{19}$$

The value for across-track repositioning is then given as:

$$\Delta\hat{y}_{1,redisp} = -\Delta\hat{y}_1 = -\frac{\sin\theta_{i,1}}{\lambda \hat{k}_{a,1}}\hat{v}_{y1}{}^2 . \tag{19}$$

By rewriting equation (3) the estimate of the along-track velocity is obtained:

$$\hat{v}_{x1} = v_p - \sqrt{-\hat{k}_{a,1}\frac{\lambda r_1}{2} - y_1 \hat{a}_y} . \tag{17}$$

By rewriting equation (9) the along-track distance traveled by the target can be computed:

$$\Delta\hat{x}_b = \Delta\hat{x}_{img} - v_p \frac{2 \sin\theta_{i,1}}{\lambda \hat{k}_{a,1}}\hat{a}_y \Delta t_b \tag{18}$$

The along-track acceleration can then be expressed by rewriting equation (5):

$$\hat{a}_x = \frac{2}{\Delta t_b{}^2}\left(\Delta\hat{x}_b - \hat{v}_{x1}\Delta t_b\right) \tag{18}$$

IV. Estimation Accuracy and Errors

One of the most important steps for traffic monitoring applications is the repositioning of the detected targets to their true broadside position. Only with the knowledge of the true position the moving target can be assigned to a certain road and traffic management becomes feasible.

Using only a single satellite with two apertures (e.g. TerraSAR-X) and computing the repositioning values for the moving targets only from the along-track interferometric (ATI) phases, high errors in the order of several hundreds of meters may occur due to ATI phase noise and clutter interference. To reduce these errors the complex incorporation of a road database and a-priori knowledge into the estimation step is necessary [9].

In the following it is shown, that our proposed approach allows the along-track repositioning of moving targets with high accuracy without a-priori knowledge and without having a road database. Nevertheless, a road database would allow to further increase the estimation accuracy.

If the SCNR is high enough for detecting and focusing the target in the clutter suppressed DPCA image, we assume that the estimation error of the relative along-track displacement for the two-dimensional correlation process (cf. Fig. 3) is constant and in the order or even smaller than one azimuth resolution cell. For a first estimation we set: $\sigma_{\Delta\hat{x}_{img}}$ = 3 m.

For the proposed method the along-track repositioning error for a first preliminary estimation can be approximated as (for this preliminary investigation the influence of clutter or SNCR, respectively, is not considered):

$$\sigma_{\Delta\hat{x}_{1,redisp}} = \left|\frac{2v_p\sin\theta_{i,1}}{\lambda k_{a,1}}\right|\sqrt{\frac{v_{y1}{}^2}{k_{a,1}{}^2}\sigma^2_{\hat{k}_{a,1}} + \frac{1}{\Delta t_b{}^2}\sigma^2_{\Delta\hat{y}_{img}} + \frac{\Delta t_b{}^2}{4}\sigma^2_{\hat{a}_y}}$$

The standard deviation of the Doppler slope estimated using a maximum likelihood technique as a function of integration time T and SNR is given as [7]:

$$\sigma_{\Delta\hat{k}_{a,1}} \cong \frac{2}{T^2}\frac{1}{\sqrt{SNR}}.$$

In the following figures some preliminary error estimation results using the equations above are presented. As system and geometry parameters the values listed in table 1 were used. For the results shown in Fig. 5 it was assumed that the no target acceleration occurs. In that case, one would expect that an increase of the along-track baseline and the time lag between the observations would lead to a smaller repositioning error. However, the results shown in Fig. 6 indicate, that in presence of accelerations (in real traffic scenarios the standard deviations of accelerations of common passenger cars are in the order of 0.5 m/s² [8]) the baseline should not be increased above a certain value. For the parameters used in the error calculation the optimum value for the time lag Δt_c is somehow between 2 and 4 s, corresponding to an along-track baseline of about 15 to 30 km.

TABLE I. System and Geometry Parameters Used for Simulations

Parameters	Value
platform velocity v_p	7600 m/s
wavelength λ	0.0312284 m
pulse repetition frequency *PRF*	6500 Hz
processed bandwidth	3250 Hz
range chirp bandwidth	150 MHz
range chirp duration	28 µs
altitude above ground	514 km
incidence angle θ_i	45°

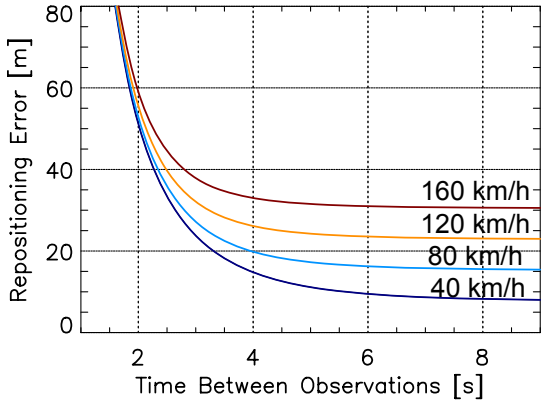

Figure 5. Across-track repositioning error as a function of time lag Δt_c for different along-track velocities (SNR = -20 dB, $\sigma_{\hat{a}_y}$ = 0 m/s²).

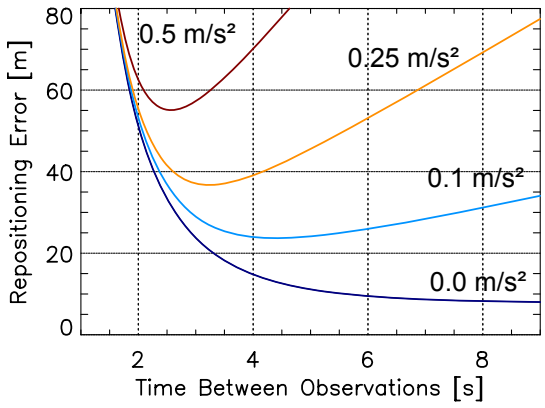

Figure 6. Across-track repositioning error as a function of time lag Δt_c for different across-track acceleration errors (SNR = -20 dB, v_{y1} = 80 km/h).

V. SIMULATIONS

To verify the equations derived in section II and the parameter estimation procedure in section III, a simulation using a SAR simulator developed at the Microwaves and Radar Institute was used. As simulation parameters the system parameters listed in table 1 were considered.

A point target moving with an absolute velocity of 130 km/h at $t = 0$ and constant acceleration of 0.5 m/s² was simulated. The position of the target in ground plane at $t = 0$ was set to $x_1 = 0$, $r_1 = 726.9$ km, $\theta_{i,1} = 45°$ ($\Rightarrow y_1 = 514$ km). The driving direction of the target with respect to the x-axis was 60° so that the along-track and across-track velocity and acceleration components of the target at $t = 0$ are: $v_{x1} = 65.000$ km/h, $v_{y1} = 112.583$ km/h, $a_x = 0.250$ m/s² and $a_y = 0.433$ m/s².

An along-track baseline d_a of 19 km corresponding to a time lag Δt_c of 2.5 s was adjusted. Both SAR images were focused using the estimated Doppler slope from the target in image 1. The focused SAR images are shown in Fig. 5.

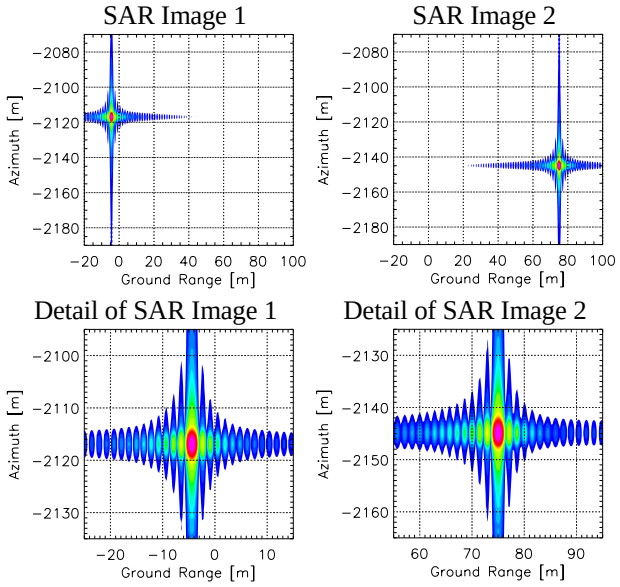

Figure 7. Co-registered SAR images obtained by platform 1 (left column) and platform 2 (right column). For visulization purposes the impulse responses were interpolated.

The estimated Doppler slope of the target in image 1 is $k_{a,1} = -5084$ Hz. The relative target displacements between both images can e.g. be determined by a two-dimensional correlation procedure. However, for a first verification of the proposed GMTI method it is sufficient to estimate the displacements manually by just comparing both images. The estimated displacements are:

$$\Delta x_{img} = \Delta x_2 - \Delta x_1 = -2145 \text{ m} - (-2117 \text{ m}) = -28.0 \text{ m},$$

$$\Delta y_{img} = \Delta y_2 - \Delta y_1 = 75 \text{ m} - (-4.5 \text{ m}) = 79.5 \text{ m}.$$

Using the estimates of the displacements and also the estimated Doppler slope, the proposed algorithm in section III delivers the following results: $a_y = 0.44$ m/s², $v_{y1} = 112.49$ km/h, $\Delta x_{1,redisp} = 2115.42$ m, $\Delta y_{1,redisp} = 4.35$ m, $v_{x1} = 67.17$ km/h, $\Delta x_b = 46.72$ m and $a_x = -0.23$ m/s².

The results are, apart from the along-track acceleration a_x, in good agreement with the true parameters of the moving target. The along-track re-positioning error is $2115.42 - 2117 \cong 1.6$ m, the across-track re-positioning error is even negligible small and the estimation errors of the velocity components are better than 2.2 km/h.

VI. CONCLUSIONS

A new method for GMTI using TerraSAR-X and TanDEM-X in an along-track configuration with a large baseline was presented and verified using a SAR GMTI simulator. The method allows the repositioning of the moving targets in the SAR images to their true broadside position with high accuracy as well as the estimation of the velocity and acceleration vectors.

During the operational phase of TanDEM-X, where as primary objective a DEM will be generated, the along-track baseline will be shorter than required for achieving the best possible GMTI performance. Nevertheless, during the commissioning phase of TanDEM-X longer baselines are feasible and so we are looking forward to apply the proposed GMTI method and to verify it using real SAR data acquired by TerraSAR-X and TanDEM-X.

REFERENCES

[1] G. Krieger et al., "TanDEM-X: Mission Concept, Product Definition and Performance Prediction," Proceedings of EUSAR 2006, Dresden, Germany.

[2] F.R. Dickey and M.M. Santa, "Final Report on Anti-Clutter Techniques," General Electric Co., Heavy Military Electron. Dept., Rep. No. R65EMH37, Syracuse, NY, 1953.

[3] H. Runge et al.," Performance Analysis of Virtual Multi-Channel Modes for TerraSAR-X," Proceedings of EUSAR 2006, Dresden, Germany.

[4] V.C. Chen and H. Ling, "Time-Frequency Transforms for Radar Imaging and Signal Analysis," Artech House, 2002.

[5] J.H.G. Ender, "The airborne experimental multi-channel SAR system AER-II," Proceedings of EUSAR 1996, Königswinter, Germany, pp. 49-52.

[6] S. Chiu and I. Sikaneta, "Applying Fractional Fourier Transform to Two-Aperture SAR-GMTI," Proceedings of EUSAR 2004, Ulm, Germany.

[7] S. Barbarossa, "Detection and imaging of moving objects with synthetic aperture radar – Part 1: Optimal detection and parameter estimation theory," IEE Proceedings-F, vol. 139, no.1, pp. 79-88, February 1992.

[8] S. Baumgartner, M. Gabele, G. Krieger, K.-H. Bethke and S. Zuev, "Traffic Monitoring with SAR: Implications of Target Acceleration," Proceedings of EUSAR 2006, Dresden, Germany.

[9] F. Meyer et al, "Towards traffic monitoring with TerraSAR-X" Canadian Journal of Remote Sensing, vol. 33, no. 1, pp.39-51, 2007.